



Luminescence properties of full-color single-phased phosphors for white LEDs

Wenbo Ma*, Zhaopu Shi*, Rong Wang

Ocean's King Lighting Science & Technology Co., Ltd., Shenzhen 518054, China

ARTICLE INFO

Article history:

Received 6 January 2010

Received in revised form 28 April 2010

Accepted 28 April 2010

Available online 5 May 2010

Keywords:

White LED

Phosphors

Full-color

Energy transfer

ABSTRACT

A series of full-color single-phased phosphors for white LEDs (W-LEDs), in the system $(Y, Ln)_2GeO_5$ ($Ln = Tm, Tb, Eu$), were prepared and their photoluminescence properties were characterized. The simultaneous incorporation of Eu^{3+} , Tb^{3+} and Tm^{3+} ions in Y_2GeO_5 lattice can result in an integration of red, green, and blue emissions when being excited by ultraviolet light. Under excitation at 352 nm, the color tones of the $(Y_{0.95-x}Tm_{0.01}Tb_xEu_{0.04})_2GeO_5$ phosphors change from cool white to warm white by increasing the concentration of Tb^{3+} , while the intensities of Eu^{3+} emissions increase. Indeed, in the case of co-doped systems, a very efficient energy that transfers from Tb^{3+} to Eu^{3+} occurs. The present phosphors can potentially be used for the high CRI and high luminous efficient white LEDs.

© 2010 Elsevier B.V. All rights reserved.

1. Introduction

In recent years, there has been an increasing trend for white light emitting diodes (W-LEDs) to replace the conventional incandescent and fluorescent lamps, due to their long lifetime, high energy efficiency, environmental protection and so on. At present, W-LEDs are fabricated by combining one or two different types of phosphors that can be excited by the blue LED chip [1]. However, white LED with yellow YAG:Ce phosphor excited by blue GaN has the following problems: white emitting color changes with input power, the mix-up of the two colors results in low color rendering index and strong dependence of white color quality on an amount of phosphor leads to low reproducibility [2,3]. In order to overcome these problems, it is essential to explore novel and efficient full-color luminescent materials that can directly emit white light under the excitation from the ultraviolet LED chip [4]. Recently, a lot of attention has been paid to single-phased white light emitting phosphors [5–8], which have a large potential application for white light LED. In these systems, the performance of white LEDs, including the CRI, color temperature, and color range, will significantly depend on the employed phosphors [9]. In this work, unusual full-color phosphors with simultaneous incorporation of Tm^{3+} (blue), Tb^{3+} (green) and Eu^{3+} (red) in the lattice of Y_2GeO_5 are described, which could lead to single-phased white light emitting phosphors. In particular, the dependence of luminescence properties on the concentration of R-G-B Ln^{3+} ions is discussed.

2. Experimental

2.1. Synthesis

$(Y, Tm, Tb, Eu)_2GeO_5$ materials were synthesized by solid-state reaction method. The starting materials used were highly pure Y_2O_3 (Griem, 99.99%), GeO_2 (SCRC, 99.99%), Tm_2O_3 (Griem, 99.99%), Tb_4O_7 (Griem, 99.99%), and Eu_2O_3 (Griem, 99.99%). Stoichiometric amounts of starting materials were ground well and fired at 1350 °C for 12 h in air and then cooled to room temperature (RT) in the furnace, and then the powder samples can be used.

2.2. Characterization

The X-ray diffraction (XRD) of the powder samples was examined by a Rigaku-Dmax 2500 diffractometer using $Cu K\alpha$ radiation ($\lambda = 0.15405$ nm). Photoluminescence spectra were measured by a Shimadzu Spectrofluorophotometer RF-5301PC. The lifetime spectra were measured by Fluorescence Spectrometer FLS920. The photoluminescence and lifetime spectra were recorded at room temperature. The particle size is measured by Malvern Mastersize 2000 Laser Analyzer.

3. Results and discussion

The X-ray diffraction patterns of $(Y, Ln)_2GeO_5$ ($Ln = Tm, Tb, Eu$) samples with different Ln ions are shown in Fig. 1a. From Fig. 1a we can see that single phase of Y_2GeO_5 (PDF No. 23-1484 [10]) was obtained for the samples synthesized at 1350 °C. No second phase was detected, as indicates that, at the doping level used, the Tm^{3+} , Tb^{3+} , Eu^{3+} can be completely dissolved in the Y_2GeO_5 host lattice by substitution for the Y^{3+} . The distribution of particle size for $(Y_{0.96}Eu_{0.04})_2GeO_5$ sample as shown in Fig. 1b demonstrated that the obtained particle size was about 8 μm .

Fig. 2 shows the RT emission and excitation spectra of $(Y_{0.99}Tm_{0.01})_2GeO_5$, $(Y_{0.96}Tb_{0.04})_2GeO_5$ and $(Y_{0.96}Eu_{0.04})_2GeO_5$ samples. The inset of Fig. 2 shows the excitation spectra

* Corresponding authors. Tel.: +86 755 26588815; fax: +86 755 26588821.
E-mail addresses: ma.wenbo1978@hotmail.com (W. Ma),
shizhaopu0924@163.com (Z. Shi).

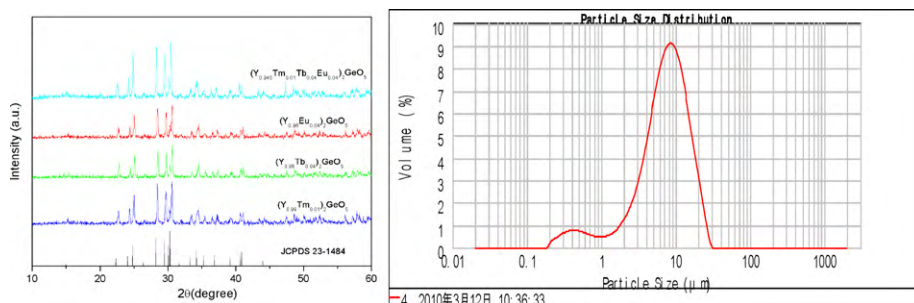


Fig. 1. (a) XRD patterns of $(Y, Ln)_2GeO_5$ ($Ln = Tm, Tb, Eu$) samples. The standard data for Y_2GeO_5 are shown as references. (b) The particle size distribution of $(Y_{0.96}Eu_{0.04})_2GeO_5$ sample.

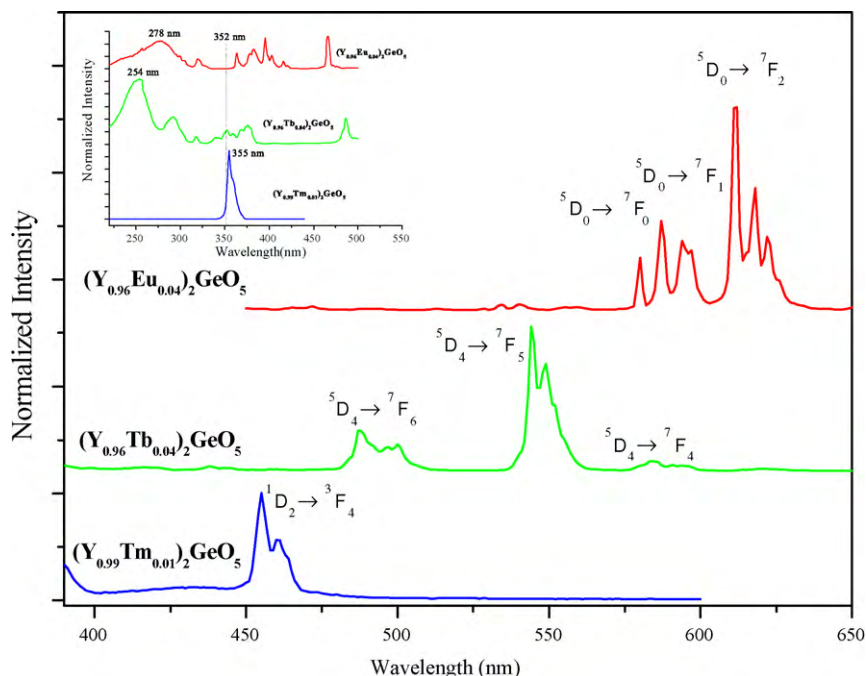


Fig. 2. RT emission spectra of $(Y_{0.99}Tm_{0.01})_2GeO_5$, $(Y_{0.96}Tb_{0.04})_2GeO_5$ and $(Y_{0.96}Eu_{0.04})_2GeO_5$ samples, under excitation at 355(Tm³⁺), 376(Tb³⁺), 396 (Eu³⁺) nm.

of $(Y_{0.99}Tm_{0.01})_2GeO_5$, $(Y_{0.96}Tb_{0.04})_2GeO_5$ and $(Y_{0.96}Eu_{0.04})_2GeO_5$ samples at room temperature, monitored within the Eu³⁺ $^5D_0 \rightarrow ^7F_2$ (611 nm), Tb³⁺ $^5D_4 \rightarrow ^7F_5$ (544 nm), and Tm³⁺ $^1D_2 \rightarrow ^3F_4$ (455 nm) emission transitions, respectively. For $(Y_{0.96}Eu_{0.04})_2GeO_5$, the strongest excitation peak is at 396 nm. The emissions of Eu³⁺ in the vicinity of 600 nm are due to the magnetic dipole transition $^5D_0 \rightarrow ^7F_{0-1}$, which is insensitive to the site symmetry [2,11,12]. The emission around 610–630 nm is due to the electric dipole transition of $^5D_0 \rightarrow ^7F_2$, induced by the lack of inversion symmetry at the Eu³⁺ site, and is much stronger than that of the transition to the 7F_1 state. On the photoluminescence spectrum of $(Y_{0.96}Tb_{0.04})_2GeO_5$, the strongest excitation peak is at 254 nm, and emission occurs from 480 nm to 610 nm and is due to $^5D_4 \rightarrow ^7F_{4-6}$ transitions for Tb³⁺ [13,14]. Among the emission lines from 5D_4 state, the $^5D_4 \rightarrow ^7F_5$ emission line at approximately 544 nm is the strongest. The reason is that there is the greatest probability of the transition for both electric-dipole and magnetic-dipole induced transition. Under the excitation at 355 nm, which is the strongest excitation peak, the $(Y_{0.99}Tm_{0.01})_2GeO_5$ phosphor exhibits the characteristic emission of Tm³⁺ (blue line) at 455 nm which corresponds to the transition of Tm³⁺ from 1D_2 to 3F_4 . This blue $^1D_2 \rightarrow ^3F_4$ emission is quite sharp, with a full width at half maximum of about 10 nm.

Fig. 3 gives the RT emission spectra of the $(Y_{0.95-x}Tm_{0.01}Tb_xEu_{0.04})_2GeO_5$ ($x = 0.01, 0.02, 0.04, 0.06, 0.08$)

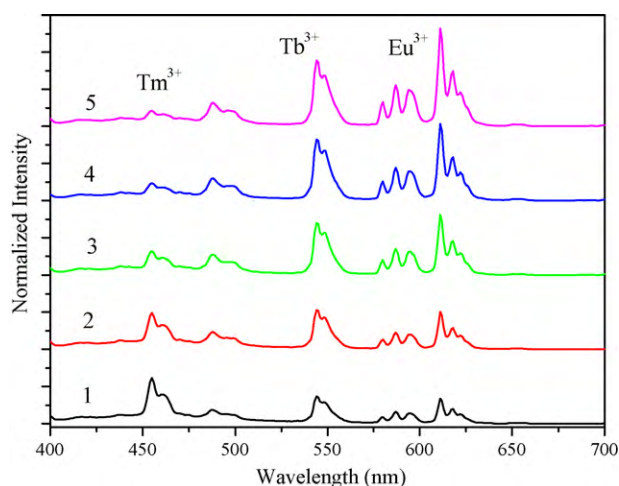


Fig. 3. RT emission spectra of the phosphors excited by 352 nm. 1, $(Y_{0.94}Tm_{0.01}Tb_{0.01}Eu_{0.04})_2GeO_5$; 2, $(Y_{0.93}Tm_{0.01}Tb_{0.02}Eu_{0.04})_2GeO_5$; 3, $(Y_{0.91}Tm_{0.01}Tb_{0.04}Eu_{0.04})_2GeO_5$; 4, $(Y_{0.89}Tm_{0.01}Tb_{0.06}Eu_{0.04})_2GeO_5$; 5, $(Y_{0.87}Tm_{0.01}Tb_{0.08}Eu_{0.04})_2GeO_5$.

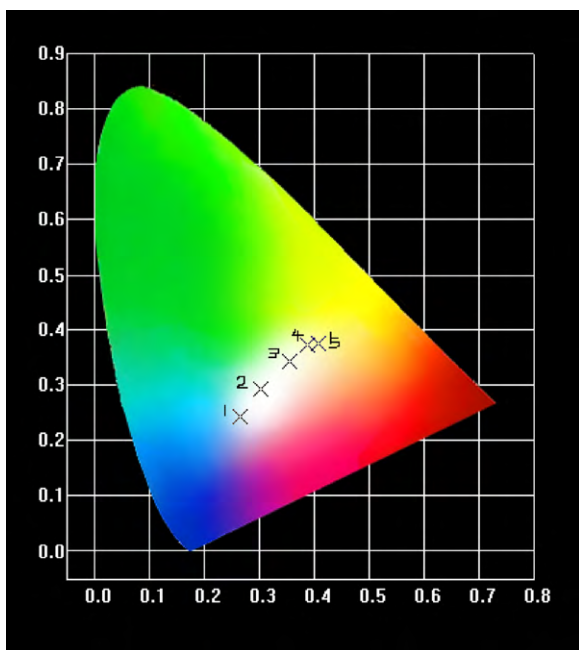


Fig. 4. CIE chromaticity diagram for the phosphors. 1, $(Y_{0.94}Tm_{0.01}Tb_{0.01}Eu_{0.04})_2GeO_5$; 2, $(Y_{0.93}Tm_{0.01}Tb_{0.02}Eu_{0.04})_2GeO_5$; 3, $(Y_{0.91}Tm_{0.01}Tb_{0.04}Eu_{0.04})_2GeO_5$; 4, $(Y_{0.89}Tm_{0.01}Tb_{0.06}Eu_{0.04})_2GeO_5$; 5, $(Y_{0.87}Tm_{0.01}Tb_{0.08}Eu_{0.04})_2GeO_5$.

phosphors with different Tb-doped levels under excitation at 352 nm. For an excitation at 352 nm (this nicely matches the requirements for W-LEDs) a full-color emission is obtained, resulting from the simultaneous red, green, and blue emission of Eu^{3+} , Tb^{3+} , and Tm^{3+} ions in Fig. 3. With the Tb^{3+} ion concentration increasing, the intensities of Tb^{3+} green emissions and Eu^{3+} red emissions increase. The corresponding chromaticity coordinates are represented in the CIE diagram of Fig. 4. In the $(Y_{0.95-x}Tm_{0.01}Tb_xEu_{0.04})_2GeO_5$ phosphors, the color tones change from cool white (which is represented at point 1) to warm white (which is represented at points 4 and 5) by adjusting the concentrations of Tb^{3+} , such as for $(Y_{0.94}Tm_{0.01}Tb_{0.01}Eu_{0.04})_2GeO_5$, $(Y_{0.93}Tm_{0.01}Tb_{0.02}Eu_{0.04})_2GeO_5$, $(Y_{0.91}Tm_{0.01}Tb_{0.04}Eu_{0.04})_2GeO_5$, $(Y_{0.89}Tm_{0.01}Tb_{0.06}Eu_{0.04})_2GeO_5$,

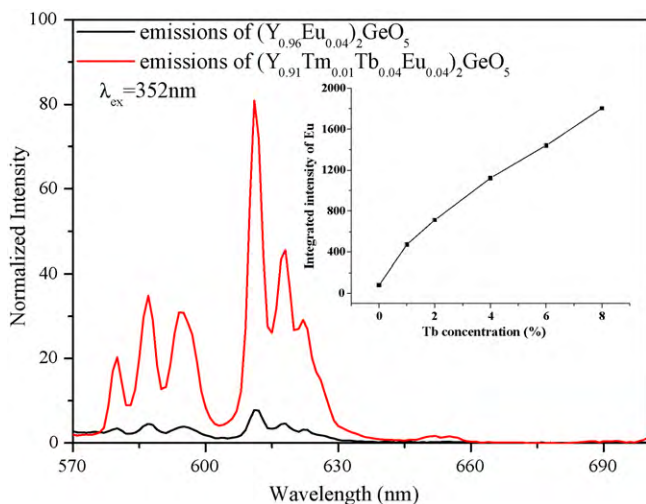


Fig. 5. Emission spectra of $(Y_{0.96}Eu_{0.04})_2GeO_5$ and $(Y_{0.91}Tm_{0.01}Tb_{0.04}Eu_{0.04})_2GeO_5$ under excitation at 352 nm; the inset shows the effect of Tb^{3+} concentration on the integrated intensities of Eu^{3+} emissions from 570 nm to 640 nm.

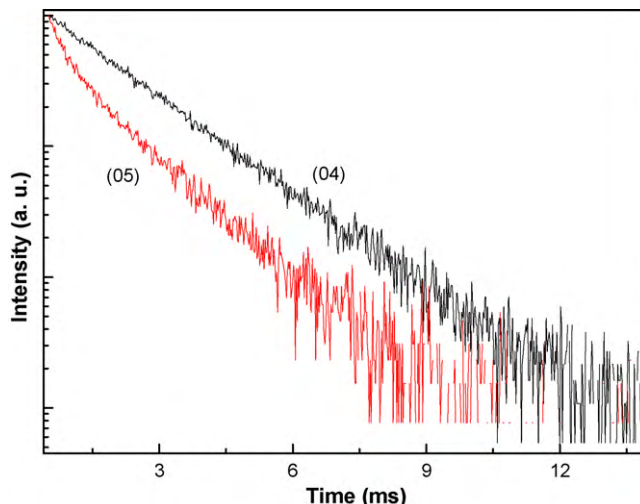


Fig. 6. Decay curves of Tb^{3+} at 544 nm in $(Y_{0.96}Tb_{0.04})_2GeO_5$ (04) and $(Y_{0.91}Tm_{0.01}Tb_{0.04}Eu_{0.04})_2GeO_5$ (05).

and $(Y_{0.87}Tm_{0.01}Tb_{0.08}Eu_{0.04})_2GeO_5$; the corresponding chromaticity coordinates are (0.2651, 0.2421), (0.3026, 0.2924), (0.3556, 0.3431), (0.3865, 0.3713), and (0.4085, 0.3749), respectively.

Fig. 5 gives the emission spectra of $(Y_{0.96}Eu_{0.04})_2GeO_5$ and $(Y_{0.91}Tm_{0.01}Tb_{0.04}Eu_{0.04})_2GeO_5$ under excitation at 352 nm. Under selective excitation of Tb^{3+} ions, at 352 nm, emission from Eu^{3+} ions in $(Y_{0.96}Eu_{0.04})_2GeO_5$ is very weak. But the integrated intensity from 570 nm to 640 nm originating from Eu^{3+} ions was found to increase in $(Y_{0.91}Tm_{0.01}Tb_{0.04}Eu_{0.04})_2GeO_5$ by a factor of about 14.0. And with the Tb^{3+} concentration (x) changing from 0.01 to 0.08 in the $(Y_{0.95-x}Tm_{0.01}Tb_xEu_{0.04})_2GeO_5$ phosphors, the integrated intensities of Eu^{3+} emissions from 570 nm to 640 nm also increase from 6 times to 22.5 times as that of $(Y_{0.96}Eu_{0.04})_2GeO_5$ (see the inset in Fig. 5). This enhancement could be due to an energy transfer from Tb^{3+} to Eu^{3+} .

Additional experimental support on efficient energy transfer from Tb^{3+} to Eu^{3+} came from the lifetime measurements. Fig. 6 gives decay curves of Tb^{3+} f-f transition at 544 nm for different Eu^{3+} concentrations. The lifetime for Tb^{3+} emission at 544 nm in $(Y_{0.91}Tm_{0.01}Tb_{0.04}Eu_{0.04})_2GeO_5$ is 1.17 ms, whereas it is 1.75 ms in $(Y_{0.96}Tb_{0.04})_2GeO_5$. An energy transfer efficiency of 33% could be

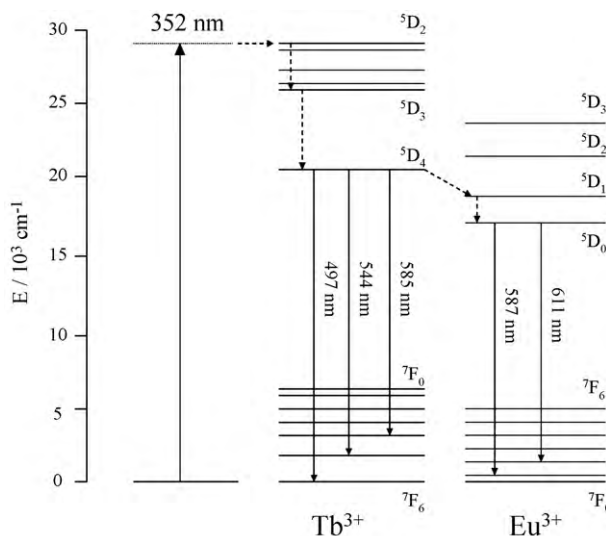


Fig. 7. Energy diagram of Tb^{3+} and Eu^{3+} in $(Y_{0.91}Tm_{0.01}Tb_{0.04}Eu_{0.04})_2GeO_5$.

estimated through $\eta(ET) = 1 - k_D/k_{AD}$, k_D represents the decay rate in the absence of the acceptor (Eu^{3+}) and k_{AD} represents the decay rate in the presence of the acceptor [15].

Excitation of Eu^{3+} can occur much easily via energy transfer from the $\text{Tb}^{3+} \text{ } ^5\text{D}_4$ to the $\text{Eu}^{3+} \text{ } ^5\text{D}_1$ states when pumped with 352 nm. After excitation of the $\text{ } ^5\text{D}_2$ state of Tb^{3+} , the electrons relax non-radiatively to the $\text{ } ^5\text{D}_4$ state of Tb^{3+} , and then some electrons relax radiatively to the $\text{ } ^7\text{F}_5$ and $\text{ } ^7\text{F}_4$ state of Tb^{3+} , emitting at 544 nm and 585 nm, while some electrons are transferred to the $\text{ } ^5\text{D}_1$ level of Eu^{3+} . Then, the electrons in $\text{ } ^5\text{D}_1$ level relax, firstly, through non-radiatively decay to $\text{ } ^5\text{D}_0$ levels and, next, decay to the $\text{ } ^7\text{F}_1$, emitting at 587 nm, or to the $\text{ } ^7\text{F}_2$, emitting at 611 nm. Energy level diagram as shown in Fig. 7 gives clearly process of the luminescence mechanism, which is quantitatively confirmed by the 3-level model for energy transfer [16,17].

4. Conclusions

In summary, $(\text{Y, Ln})_2\text{GeO}_5$ ($\text{Ln} = \text{Tm, Tb, Eu}$) materials were synthesized by solid-state reaction method. Under excitation by UV light, the emission of red (Eu^{3+}), green (Tb^{3+}), and blue (Tm^{3+}) light were observed, and the color tones of $(\text{Y}_{0.95-x}\text{Tm}_{0.01}\text{Tb}_x\text{Eu}_{0.04})_2\text{GeO}_5$ changed from cool white to warm white by adjusting the Tb^{3+} concentration. In addition, in the case of co-doped systems, energy transfer occurred from Tb^{3+} to Eu^{3+} and Tb^{3+} ion can be regarded as a sensitizer. The white light generates when a UV-LED illuminates these $(\text{Y}_{0.95-x}\text{Tm}_{0.01}\text{Tb}_x\text{Eu}_{0.04})_2\text{GeO}_5$ phosphors, which, to some

extent, will simplify greatly the usage of the present phosphor.

Acknowledgement

The research was supported by Ocean's King Lighting Science & Technology CO. Ltd.

References

- [1] Z.Y. Lin, X.L. Liang, Y.W. Ou, C.X. Fan, S.L. Yuan, H.D. Zeng, G.R. Chen, *J. Alloys Compd.* 496 (2010) L33.
- [2] L. Zhou, J. Wei, J. Wu, F. Gong, L. Yi, J. Huang, *J. Alloys Compd.* 476 (2009) 390.
- [3] C.F. Guo, Y. Xu, F. Lv, X. Ding, *J. Alloys Compd.* 497 (2010) L21.
- [4] T. Nishida, T. Ban, N. Kobayashi, *Appl. Phys. Lett.* 82 (2003) 3817.
- [5] X.D. Qi, C.M. Liu, C.C. Kuo, *J. Alloys Compd.* 492 (2010) L61.
- [6] C.H. Liang, Y.C. Chang, Y.S. Chang, *Appl. Phys. Lett.* 93 (2008) 211902.
- [7] B.V. Rao, K. Jang, H.S. Lee, S.S. Yi, J.H. Jeong, *J. Alloys Compd.* 496 (2010) 251.
- [8] K.H. Kwon, W.B. Im, H.S. Jang, H.S. Yoo, D.Y. Jeon, *Inorg. Chem.* 48 (2009) 11525.
- [9] C.H. Liang, Y.C. Chang, Y.S. Chang, *Appl. Phys. Lett.* 93 (2008) 211902.
- [10] ICDD-International Center for Diffraction Data, Card No. 23-1484.
- [11] X.X. Zhao, X.J. Wang, B.J. Chen, Q.Y. Meng, B. Yan, W.H. Di, *Opt. Mater.* 29 (2007) 1680.
- [12] X.M. Liu, J. Lin, *J. Appl. Phys.* 100 (2006) 124306.
- [13] M. Laroche, J.L. Doualan, S. Grard, J. Margerie, R. Moncorge, *J. Opt. Soc. Am. B* 17 (2000) 1291.
- [14] L. Van Pieterson, M.F. Reid, G.W. Burdick, A. Meijerink, *Phys. Rev.* 65 (2002) 45114.
- [15] T.S. Chernaya, L.A. Muradyan, V.A. Sarin, E.M. Uyukin, Kh.S. Bagdasarov, V.I. Simonov, *Kristallografiya* 34 (1989) 1295.
- [16] M.V. Nazarov, D.Y. Jeon, J.H. Kang, E.-J. Popovici, L.-E. Muresan, M.V. Zamoryanskaya, B.S. Tsukerblat, *Solid State Commun.* 131 (2004) 307.
- [17] M.V. Nazarov, B.S. Tsukerblat, E.-J. Popovici, D.Y. Jeon, *Solid State Commun.* 133 (2005) 203.